

EXPERIMENTAL DETERMINATION OF SATELLITE BOLTED JOINTS THERMAL
RESISTANCE

Marcia Barbosa Henriques Mantelli and José Edson Basto
Brazilian Institute for Space Research

1060184

ABSTRACT

The main objective of this work is to determine experimentally the thermal resistance of the bolted joints of the first Brazilian satellite (SCD1). These joints, used to connect the satellite structural panels, are reproduced in an experimental apparatus, keeping, as much as possible, the actual dimensions and materials. A controlled amount of heat is forced to pass through the joint and the difference of temperature between the panels is measured. The tests are conducted in a vacuum chamber with liquid nitrogen cooled walls, that simulates the space environment. Experimental procedures are used to avoid much heat losses, which are carefully calculated. Important observations about the behaviour of the joint thermal resistance with the variation of the mean temperature are made. All the experimental work is developed in the Brazilian Institute for Space Research Thermal Control Laboratory.

INTRODUCTION

The determination of bolted joint thermal resistance is very important for satellite temperature distribution calculations. In the first Data Collection Brazilian Satellite (SCD1), where only thermal control passive methods are used, the bolted joints between structural panels are of primary importance in the satellite thermal design. The heat conducted by the satellite panels and/or their electronic boxes depends on the joints' thermal resistance values, so they are projected taking into account thermal and structural considerations.

The theoretical calculation of the thermal resistance is very difficult, because it depends on a series of factors like:

- shape and physical properties of junction materials,
- type and material of bolts,
- materials and number of washers,
- joint aperture strength,
- thermal contact resistance between: washers, bolts and washers, bolts and panels, washers and panels, etc.

The numerical determination of this thermal resistance, using nodal modelling technic, is also hard to do because all the physical properties must be well known before making the calculations (frequently these data, or the measurement equipment, are not available).

An always useful procedure, that is adopted in this work, is to obtain this resistance by experimental simulation of the bolted joints. The satellite junctions are reproduced and tested in a vacuum chamber with liquid nitrogen cooled walls, in the Satellite Thermal Control Laboratory of the Brazilian Institute for Space

Research (INPE). Some series of tests were performed at INPE, but only the last one, with the best results, is described here.

SATELLITE BOLTED JOINTS

There are several types of junctions in the SCD1 satellite, but only the joints placed between the external vertical and the central horizontal structural panels are studied. In the central panel many dissipating equipment are installed. They are connected to the external vertical panels by two types of junctions: one with blind threaded insert (where the nut is fixed) and the other with a floating nut insert. Their positions in the satellite and the studied junctions schematic views are shown in the figure 1. Some electronic boxes are fixed to the horizontal panel by junctions very similar to these ones, so that the resistance obtained in this work can be used in the thermal control design of the satellite electronic equipment.

The described joints fasten two 2024 aluminum (ANSI standard) panel closing sheets (thickness: 2 and 1 mm, see figure 1), to the honeycomb panel inserts. For the panels' thermal insulation, two 1.6 mm thick epoxy+fiberglass intercalated by a 0.4 mm thick stainless steel washers, are used between the insert and the aluminum sheet. An epoxy+fiberglass washer is in contact with the insert, and a stainless steel one, with the closing sheets. The epoxy+fiberglass and stainless steel washers are present between the bolt head and the aluminum sheet either. The washers' materials were chosen to satisfy the thermal (epoxy+fiberglass) and structural (stainless steel) requirements. The washers have external diameter of 10 mm; their internal diameters are 5 mm for the fixed nut insert joints, and 4.5 mm for the floating ones. As they do not have standard sizes, they were fabricated specially for the SCD1. The bolts used are made of titanium and have two different sizes, according to the insert type: #10 (see ASA standard) for fixed, and #8 for the floating nut insert.

EXPERIMENTAL SIMULATION

The objective of the experimental work is to measure the thermal resistance of the two types of bolted joints described in the previous section. So, the experimental apparatus were designed to reproduce, in the laboratory, the same thermal conditions found in the satellite. To enable data statistical treatment, ten similar joints are mounted for each junction and tested simultaneously. The mean resistance values and the associated standard errors (the range of values) are calculated. To study the joints behaviour with the variation of the temperature, five levels of temperature are adopted. All the tests are made in steady state conditions. It is supplied a controlled amount of heat to each apparatus, the temperatures are left to stabilize and heat flow and temperature measurements are done. The ratio between closing aluminum sheets and insert temperature difference (see figure 1), and the heat flux through the bolts and washers determines the thermal resistance of the joint.

The tests are made in the experimental facilities of the Brazilian Institute for Space Research Thermal Control Laboratory. It is used an inside volume 1 meter X 1 meter vacuum chamber with liquid nitrogen (LN₂) cooled walls. This chamber operates in high vacuum (10^{-7} Torr), with wall temperatures of -190 Centigrades. An acquisition and control data system is used to control the temperatures in levels previously established, and to store the temperature and voltage data. A PC

microcomputer program controls the experiment, through a GPIB interface and the data is recorded in its hard disk.

APPARATUS DESCRIPTION

The joints' experimental thermal simulation is made by two types of apparatus, corresponding to the two different junctions described in the previous section.

In the apparatus design, to reproduce the thermal and physical characteristics of the actual bolted joints, it was first necessary to analyse the heat flow lines across the junction components. Supposing the heat coming from the vertical panel to the horizontal panel (see figure 1), there is first a concentration of heat flow lines in the bolt direction. Then, the heat flows through two main paths: across the bolt and across the washers. The heat arrives to the insert, passes through the silicone glues that fastens the insert to the honeycomb panel, and finally reaches the horizontal panel. The value of the effective honeycomb panel thermal conductivity is very low if compared with the conductivity of the insert material, and, as all the external insert surfaces are in contact with the epoxy glue, it is considered that the heat flux rate is the same in all directions. Note that, as the floating nut insert joints have more surfaces in contact (see figure 1), it is expected a thermal resistance value bigger than the fixed nut insert one. To force the heat to flow through the washers and bolts, each apparatus has a heat source and a heat sink, with their temperatures measured by copper/constantan thermocouples. figure 2 shows a schematic view and thermocouples' localizations of the experimental apparatus for the fixed nut insert joint, while figure 3, shows them for the floating one.

The washers and their arrangements are equivalent to the actual satellite joints. As the titanium bolts were not available for testing, they are substituted by high alloy steel ones.

The closing aluminum sheets, working as heat sources, are replaced by plan heaters, made of two circular 80mm diameter 2024 aluminum sheets, 1 and 1.5 mm thick. Between the aluminum plates there is a Nickel-Chrome resistive wire (resistivity of 30 Ohms/meter), rolled in a plan spiral, electrically insulated by two 25 microns thick Polyester films. The total resistance achieved in each heater is between 15.5 and 19.0 Ohms. The heater aluminum sheets were chosen so that the total thickness value is almost the same of the joints' closing sheets. The heater size and shape was designed to simulate the effect of the radial heat flow lines in the direction of the bolt, near the joint.

Only the inserts are considered in the simulation of the honeycomb panels, as the stainless steel's conductivity is higher than those of the epoxy glue and of the honeycomb panel. They work as heat sinks (coolers), and have some of their dimensions different for the two types of the analysed junctions. They are made of the actual joints' material (stainless steel) and have a 60 mm thin circular black painted base (2mm thick) to favor the heat transfer to chamber environment. Without this base, it would not be possible to generate a well measurable heat quantity, because this dissipation would make the apparatus very hot, the difference of temperature between the heater and the cooler very small, and the measurements' uncertainties too large.

The total cooler height is 9.5 mm for the fixed nut insert and the diameter of its main body is 14.2 mm. In the center of the main body there is a screw thread hole for a #10 screw. A thermocouple is installed in the heater to measure its temperature, in a region where the heat flux has not reached the bolt and/or washers. The insert

thermocouple is installed in a point considered as the mean heat flux path (see figure 2).

The floating nut insert is simulated by a 9.4 mm diameter cylinder with a #8 screw thread hole and a 15.4 mm diameter (1 mm thick) larger basis that interacts with the insert main body when the joint is fastened (see figure 3). The main body have a 17.4 mm diameter and a 9.4 mm height cylinder. Closing the main body, soldered in the top of the cylinder, there is a thin plate with a central hole slightly larger than the screw main body diameter. The heater thermocouple is in the same position as in the fixed nut insert apparatus. The cooler thermocouple is positioned near the insert base, in a region that is considered the mean heat flux path, since the heat conducted by the joint must pass through the contact between the nut and the insert body to reach the horizontal panel.

The ten similar apparatus constructed for the two types of bolted joints, are mounted in a Celeron table (heat insulating material), according to the figure 4. They are positioned in the table to avoid the interaction among the specimens in a way that all the apparatus coolers can see the chamber environment with the same view factor, i.e. around 1. The electrical wires of five apparatus heaters are connected in series and the four resulting rows are connected in parallel. In these lateral junctions two other big wires that connect the specimens' electrical wires to the vacuum chamber wall feed through are soldered, to feed all the specimens with only one power generator.

MOUNTING PROCEDURES TO AVOID HEAT LOSSES

Some past experiments showed that the heat losses must be well controlled to warrant small experimental results' uncertainties.

To avoid the heat loss to chamber walls, and direct radiant heat exchange between the heater and the cooler, multilayer thermal insulators (MLI) in heaters' both faces are installed. The external (lower) MLI has ten layers and the internal one, that has a central hole to fit the washers and bolt, eight.

As the thermocouples and electrical wires work as fins and dissipate part of the heat by radiation, they are wrapped up with aluminized mylar to lower the surface emissivity. Their original surfaces emissivities were big, causing too much heat losses.

All the external cooler faces are black painted to force the heat to pass through the joint, excepting the internal face that is polished, to insulate the cooler and the heater from the radiation exchange .

RESULTS

To study the joint temperature variation behaviour, five levels of heater and cooler mean temperatures are used in the experimental tests. Some data resulting from tests with detected problems like: breaking of thermocouples wires, bad positioning of the copper-constantan soldered junctions, bad electrical contact between the extension wires and thermocouples or feed through, etc, were not used.

The thermal joint resistance is calculated by the following equation:

$$R = \frac{\Delta T}{Q} \quad (1)$$

where:

R : thermal joint resistance, $^{\circ}\text{C}/\text{W}$,
 ΔT : temperature difference between heater and cooler, $^{\circ}\text{C}$,
 Q : net heat flux in the joint, W.

The net heat flux is calculated through the equation:

$$Q = Q_P - Q_L \quad (2)$$

Where:

Q_P = heater dissipated power, W,
 Q_L = summation of all heat losses, W.

The heater dissipation power is determined by each heater electrical resistance and the electrical current that flows through it. The electrical resistance is directly measured (before the tests' beginning), and the current is obtained from the electrical power generator output. The following equation is used:

$$Q_P = (V/R_{eq})^2 R_e \quad (3)$$

Where:

V = electrical power generator output, V
 R_{eq} = equivalent electric resistance (summation of resistances connected in series), Ohms,
 R_e = heater electric resistance, Ohms.

All the heat losses must be carefully calculated to determine the net heat flux through the joint, as it will be discussed in the next section.

For the five temperature levels tested, the system was left for near one hour in the steady state condition. During this period, more than one hundred data were obtained at equal time intervals for each thermocouple, to verify the temperatures, presumably with small variations around a mean value. This procedure reduces the experimental errors in the results. To verify if there is electrical resistance dependence with the temperature variation, the resistances were measured in the experimental temperature levels, before the apparatus mounting. It was not verified any important variation, so that the electric resistance values obtained for each apparatus, are used in the data treatment.

Table 1 relates the following averages values for the equal apparatus: heater and cooler temperatures, heater power, summation of all heat losses and the thermal resistances, for the two types of bolted joints studied, in the five temperature levels.

HEAT LOSSES CALCULATIONS

Analysing the experimental apparatus, it is verified that there are four principal ways of heat losses: through the thermocouples wires, through the electrical wires, direct heat exchange between heater and cooler and through the MLI in the heater outer face. Each one of these heat losses is considered separately.

Thermocouples' Heat Losses

The thermocouples used in this experiment are made of copper and constantan wires. Each one of them is considered as a radiant fin so that the following well-known fin conduction and radiation equation are used to estimate the heat losses (see reference 1).

$$Q_w = (T_h - T_m) \tanh(mL) \sqrt{(h P K A)} \quad (4)$$

where:

$$m = \frac{\sqrt{(h P)}}{K A} \quad (5)$$

and:

$$h = \frac{\epsilon \sigma (T_h^4 - T_m^4)}{T_h - T_m} \quad (6)$$

Where:

Q_w = heat loss by the wire, W,
 T_h = heater temperature, °C,
 P = wire perimeter, m,
 K = wire thermal conductivity, W/m°C,
 A = wire transversal section area, m²,
 L = wire length, m,
 ϵ = surface emissivity,
 σ = Stefan-Boltzmann constant, w/m² K⁴.

Under the Celeron table, there is an aluminum platen where the experimental mounting is supported. T_m (°C) is the environment mean temperature, or the mean value between the wall chamber and the table or the platen temperature, depending on whether they are under or over the Celeron table.

Electrical Wires' Heat Losses

The wires can be divided in two groups, according to their lengths: the short ones, which connect the heaters, and the long ones, which connect the peripheral wires to the chamber walls (see figure 4).

Studying the first group, it was verified that, in spite of connecting two heaters of different temperatures, they work as heaters' fins, exchanging heat with the chamber and the Celeron table. The fins length is the distance between the heater and the point of minimum wire temperature; as this point is always near the wire middle they will not be calculated.

In the second group, the wires work as fins of the nearest heater. It is expected that a larger amount of heat is lost by these wires, since they are connected to the chamber walls that are cooled with LN. In both cases the heat losses depends on the heater temperature. The same thermocouples' losses equations are used in these calculations.

Heater External MLI Heat Losses

The heater external MLI is in physical contact with the Celeron table near its external perimeter (see Figures 2 and 3). In the losses' calculation two mechanisms are considered: conduction from the heater to the Celeron table, and radiation to the platen.

In the radiant losses' calculation, the effective emissivity values obtained in experimental works developed in this laboratory for MLI constructed with brazilian components are used (see reference 2). The radiant area is the same of the Celeron hole made to fit the mounted apparatus. The following Stefan-Boltzmann equation is used in these calculations:

$$Q_{MLIr} = \frac{\epsilon A_r \sigma (T_h^4 - T_p^4)}{1/\epsilon_{eff} + 1/\epsilon_p - 1} \quad (7)$$

where:

Q_{MLIr} = radiative MLI heat losses, W,
 A_r = Celeron hole area, m²,
 T_p = platen temperature, °C,
 ϵ_{eff} = effective emissivity,
 ϵ_p = platen emissivity.

Note that the expression in the denominator is the MLI and platen equivalent emissivity.

The Fourier law is used to determine the conductive heat losses:

$$Q_{MLIc} = \frac{K_{eff} A_c}{t} (T_h - T_s) \quad (8)$$

where:

Q_{MLIc} = conductive MLI heat losses, W,
 K_{eff} = effective thermal conductivity, W/m°C,
 A_c = MLI and Celeron contact area, m²,
 T_s = MLI surface temperature, °C,
 t = MLI thickness, m.

The effective thermal conductivity is calculated based on the effective emissivity value, on the MLI surface, platen and heater measured temperatures.

Direct Heat Exchange Between Heater and Cooler or Environment

The heat losses' calculation between heater and cooler and/or heater and environment, is made through the Stefan-Boltzmann equation. The view factor is determined by a finite difference program developed at INPE for satellite thermal designs. The apparatus were divided into 32 nodes. To simulate the heater internal MLI, the emissivity of the heater nodes was considered equal to the effective emissivity of the superinsulator. The following expression is used:

$$Q_{\text{rad}} = \epsilon_{\text{eff}} A_{\text{dr}} F_{\text{hc}} \sigma (T_{\text{h}}^4 - T_{\text{c}}^4) + \epsilon_{\text{eff}} A_{\text{dr}} F_{\text{hch}} \sigma (T_{\text{h}}^4 - T_{\text{ch}}^4) \quad (9)$$

where:

Q_{rad} = heater losses by radiation, W,
 A_{dr} = direct radiation area, m^2 ,
 F_{hc} = heat-cooler view factor,
 F_{hch} = heat-chamber view factor,
 T_{ch} = chamber walls temperature, $^{\circ}\text{C}$,
 T_{c} = cooler temperature, $^{\circ}\text{C}$

Heat Losses' Values

Table 1 presents the mean heat losses values, for the similar apparatus, for the five temperature levels tested.

EXPERIMENTAL ERRORS ANALYSIS

The calculation of the experimental standard errors is done based in reference 3. There are two types of data: the measured ones, that include the temperatures, voltages and electrical resistances, and the data obtained through mathematical models, like the thermal resistance and losses.

Some procedures are adopted to minimize the first type experimental errors. The heater, cooler, Celeron table and chamber temperatures are taken several times (about 100 measurements) so as to allow the calculation of mean value and the associated standard deviation. As there are small temperature variations with time in some measurements (the steady state conditions are not perfectly achieved, but in levels considered satisfactory), a linear regression to calculate the standard deviation values is used. The voltage values are taken two times together with the first and last temperature measurements. To improve results, a high precision voltmeter is used. The same procedure is used to the electrical resistance measurements.

In the second case, where the results are obtained indirectly, it is necessary to make some error propagation studies. It is considered that the experimental errors have a Gaussian distribution around their mean. The associated uncertainty is considered as two times the standard deviation, that corresponds to the 95.4% probability level. Considering that the experimental measurements are independent, the following formulation, illustrated by a simple example, is used in this work: suppose that a certain quantity U is obtained indirectly through the independent measurement of three parameters with mean values u , v and w , and with the associated standard deviation: σ_u , σ_v and σ_w . The experimental error is given by:

$$\sigma_U^2 = \sigma_u^2 \left(\frac{\partial U}{\partial u} \right)^2 + \sigma_v^2 \left(\frac{\partial U}{\partial v} \right)^2 + \sigma_w^2 \left(\frac{\partial U}{\partial w} \right)^2 \quad (10)$$

The determination of the thermal resistance values, (see equation 1) is made by the ratio of the temperature difference between the heater and cooler and the net heat flow through the joint. The temperature difference uncertainty is obtained by the square root of the heater and cooler temperature uncertainties squared summation:

$$\Delta(\Delta T) = \sqrt{(\Delta T_h^2 + \Delta T_c^2)} \quad (11)$$

To the calculation of the net heat flow equation 2 to 9 are used. To the experimental uncertainties calculations, a formulation similar to equation 10 is applied. Some measurements like surface emissivities, component materials' thermal conductivity, some temperatures, etc, useful in the heat losses calculation are not available, being estimated (like their uncertainties), by literature data or some complementary calculation.

Table 1 presents the mean uncertainties values, for the similar apparatus, for the five temperature levels tested.

STANDARD ERRORS' DETERMINATION

Ten similar apparatus for the two types of bolted joints studied (a total of twenty) are tested in each temperature level, to allow statistical data treatment, and as a consequence, the thermal resistance standard error calculation, given by the equation (see reference 4):

$$\text{standard error} = \frac{\sqrt{\text{standard deviation}}}{\text{similar apparatus number}} \quad (12)$$

Note that this value is different from the experimental uncertainties. The first refers to the experimental measurements errors and the second to the actual variation found among several similar actual bolted joints. The standard deviation is obtained from the thermal resistance values calculated for each apparatus. The associated standard error, together with the resistance mean values must be used in the satellite thermal designs.

It was applied the Chauvenet Criterion (see reference 3) in the determination of possible bad results, so that the sample 11 thermal resistances results must be rejected to the mean and standard errors calculation.

In table 1, the standard errors' values are compared with the uncertainties' averages for all the temperature levels.

GENERAL REMARKS

The thermal resistance as a function of the heater and cooler mean temperatures, for the two types of joints studied is presented in figure 5. The resistance values for the floating nut insert are always greater than those for the fixed one. This effect is expected because there are more surfaces in contact in the floating nut insert, as can be seen in the Figures 2 and 3. In the floating insert, the heat coming from the washers or bolt, must pass through the contact between the nut base (in disk format) and the insert body, to reach the honeycomb panel. In the fixed insert the heat path is simpler, since the insert and nut form the same body.

Another important observed effect is the variation of the thermal resistance with the temperature. It is more evident at low temperature levels: as the mean temperature increases, the resistance tends to a constant value. This can be explained studying the thermal properties' behaviour of the joints' components with the temperature variation. The epoxy+fiberglass washers coefficient of thermal expansion is around 59 m/m/k; for the aluminum, this property is around 22 m/m/k, and for the stainless steel this value is near 18 m/m/k. So, there are different contractions among the several joints component materials, with the mean temperature decrease, causing a relief in the contact pressure; the thermal contact resistance is highly dependent on the pressure (see reference 5). Another explanation is the thermal conductivity variation with the temperature; it is small for the metals (7% variation in 200 Centigrades for aluminum) and big for the epoxy+fiberglass material (100% variation in 50 Centigrades).

In figure 6 the thermal resistance results are presented, with the associated experimental mean errors (vertical bars) and the standard errors (dashed lines). In both inserts, it is verified that the experimental and the standard errors are equivalent for the same temperature levels. The experimental errors are always lower than the standard errors, excepting the thermal resistance of the lowest mean temperature level. This means that the experience was planned correctly; if the experimental errors were bigger than the actual joint resistance variation, it would not be possible to determine, with confidence, the mean value and its variation, to be used in satellite thermal design. In the lowest temperature level resistance, the experimental uncertainty is bigger than the standard error, so that the resistance mean and its expected variation can not be well established.

An interesting point to note is the difference of the experimental errors for the several calculated parameters. As is shown in table 1, the heat losses' calculation presents the highest experimental uncertainty level, sometimes reaching 50% of the total heat losses calculated. This happens due to the coarse estimation of some physical and thermal properties. But, as the losses are small, this uncertainty has a small propagation in the joint thermal resistance uncertainty (its value is around 0.5 to 3 %).

It must be noted that the joints thermal behaviour could be better understood if more thermocouples were installed in the experimental apparatus; this was impossible due to the heat losses' increasing, and the consequent experimental uncertainty increasing.

CONCLUSION

The main objective of this work, that is to measure experimentally the thermal resistance of the first brazilian satellite bolted joints, was achieved. The resultant data have been used in the satellite designs and the satellite thermal model tests have confirmed the joints thermal resistance accuracy. The experiment planning, the apparatus design, the number of similar bolted mountings, the procedures to avoid heat losses, are good enough to give the expected results, so that equivalent experimental works are recommended for future bolted joints' thermal resistance researches.

In spite of the fact that the experiment is specific for these junctions, its results can be extended to other types of bolted joints, by some theoretical study.

The effect of the thermal resistance variation with the temperature suggests that these joints can be used as a satellite active temperature controller. It is necessary to make more measurements in the curves' elbow regions (see figure 6) to study this effect with more precision.

Some numerical analysis of the thermal resistance of bolted joints is always important to do in these studies. An apparatus nodal division was made in past experiments for use in a satellite thermal analysis program developed at INPE, but up to date numerical data is not available. The numerical studies are simpler and cheaper, and must be used if they produce good results; the main difficulty is that all the necessary physical properties and thermal contact resistances must be well known before the numerical calculation. The main advantage of the experimental work is that all the interactions between the components of the joints are reproduced, not requiring theoretical studies, neither physical properties' measurements (if the heat losses are kept low).

FUTURE WORK

These bolted joints thermal resistance studies are complex and has just begun. Some suggested future work is planned to be done. First, it is suggested to make more measurements, using this same experimental mounting, in low temperature levels (elbow curves regions) to study the joints' thermal behaviour. A numerical analysis of the experimental apparatus, would be interesting, and it is suggested here. Another suggestion is the study of the influence of the bolted joints' individual components, as washers, bolts, etc, in the joints' thermal resistance. This can be done with this same apparatus, just varying, for instance, the number or material of washers and comparing the experimental results.

REFERENCES

1. Arpaci,V.S.: Conduction Heat Transfer. Addison-Wesley Publishing Company, 1966, pp 144-149.
2. Mantelli,M.B.H.: Multilayer Thermal Insulation Tests. Proceedings of the First World Conference on Experimental Heat Transfer, Fluid Mechanics, and Thermodynamics, sept. 4-9, 1988, Dubrovnik, Yugoslavia.
3. Moffat,R.J.: Describing the Uncertainties in Experimental Results. Experimental Thermal and Heat Science. Vol.1, 1988, pp 3-17.
4. Cox,D.R.: Planning of Experiments. Jonh Willey & Sons Inc., New York, 1958.
5. Mantelli,M.B.H., Pilchowski,H.U.: Thermal Contact Resistance - A Comparison of Methods. Edited by A.E.Bergles, Renssalaer Polytechnic Institute, Troy, New York.

TABLE 1. RESULTS

UNCERTAINTIES																
INSERT NUT TYPE	MEAN TEMPER. (°C)	TEMPERAT. (°C)		POWER DISSIP (W)	HEAT LOSSES (W)	THERMAL RESIST- (°C/W)	HEAT LOSSES (WATTS)				TEMPERAT. (°C)		HEATER POWER (WATTS)	HEAT LOSSES (WATTS)	TH. RESIST. (°C/W)	STD ERR.
		HEATER	COOLER				T.C.	ELECTR.	MLI	RADIAT.	HEATER	COOLER				
FLOAT.	0.685	35.125	-33.754	1.46290	0.0768	49.710	0.00607	0.01783	0.01540	0.03751	0.190	0.523	0.00608	0.02802	1.105	1.370
FIXED	6.216	26.495	-14.062	1.42177	1.3507	30.111	0.00556	0.01652	0.01434	0.03507	0.198	0.427	0.00590	0.02133	0.620	1.012
FLOAT.	-16.276	10.444	-42.996	0.99867	0.0490	56.402	0.00375	0.01200	0.00767	0.02617	0.264	0.289	0.00501	0.01855	1.216	1.575
FIXED	-10.995	4.698	-26.681	0.96884	0.0454	34.075	0.00347	0.01061	0.00696	0.02439	0.306	0.261	0.00486	0.01375	0.717	0.996
FLOAT.	-25.044	-1.705	-48.383	0.61250	0.0423	81.901	0.00348	0.01033	0.00672	0.02182	0.213	0.187	0.00471	0.01660	2.515	2.314
FIXED	-22.877	-9.272	-36.482	0.59528	0.0364	49.165	0.00307	0.00839	0.00558	0.01931	0.205	0.227	0.00457	0.01194	1.455	2.347
FLOAT.	-47.301	-29.168	-65.433	0.34592	0.0262	113.477	0.00199	0.00697	0.00288	0.01440	0.202	0.209	0.00295	0.01223	4.515	3.159
FIXED	-42.762	-32.526	-52.997	0.33620	0.0243	65.912	0.00185	0.00604	0.00265	0.01371	0.231	0.207	0.00286	0.00829	2.131	2.204
FLOAT.	-74.589	-61.907	-87.272	0.08371	0.0140	364.682	0.00109	0.00388	0.00117	0.00791	0.327	0.275	0.00145	0.01040	54.569	10.031
FIXED	-72.249	-65.076	-79.422	0.08136	0.0128	210.475	0.00099	0.00324	0.00106	0.00750	0.230	0.505	0.00140	0.00577	20.307	9.017

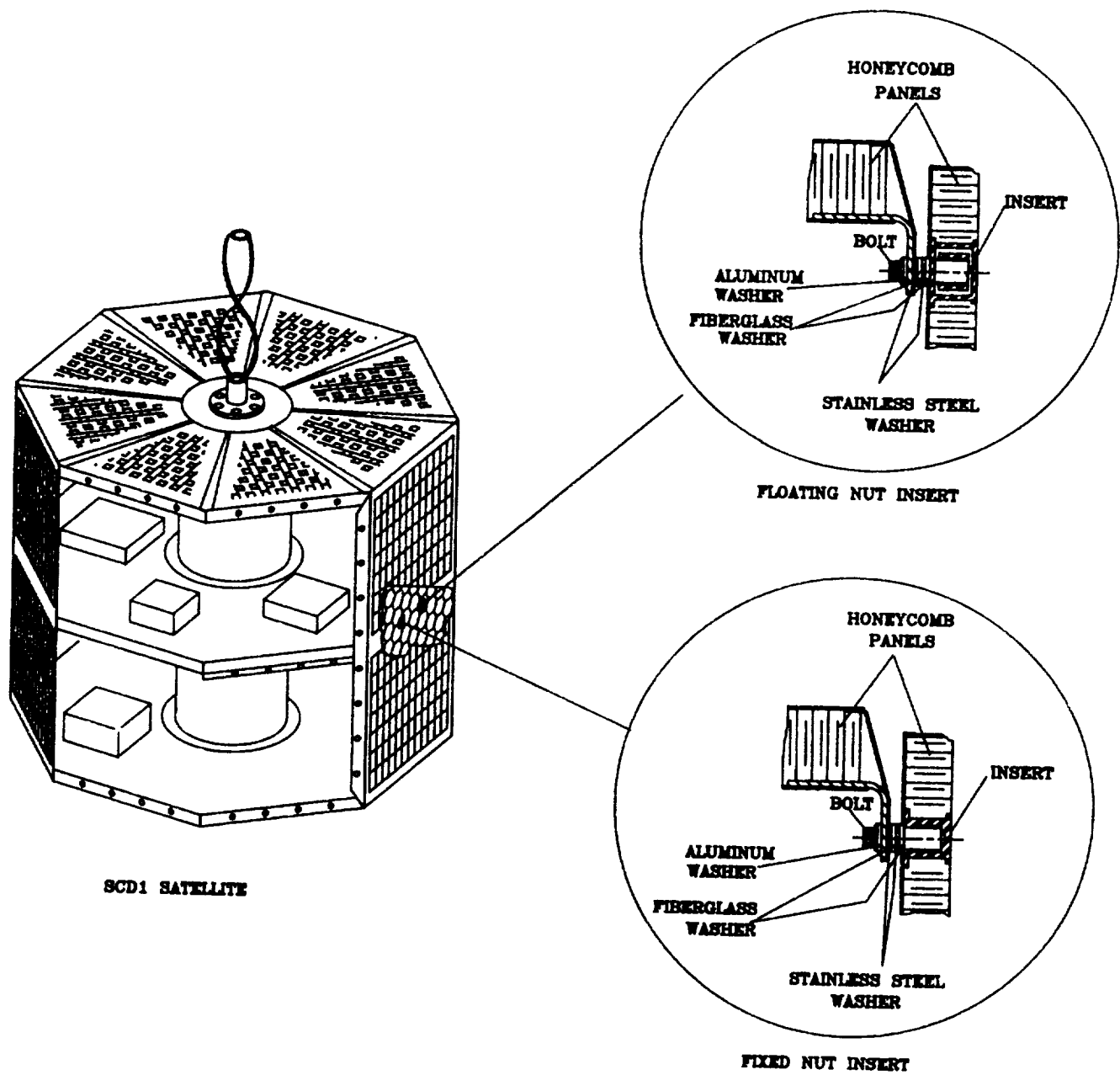


Figure 1. SCD1 schematic view, with the localization of the studied bolted joints.

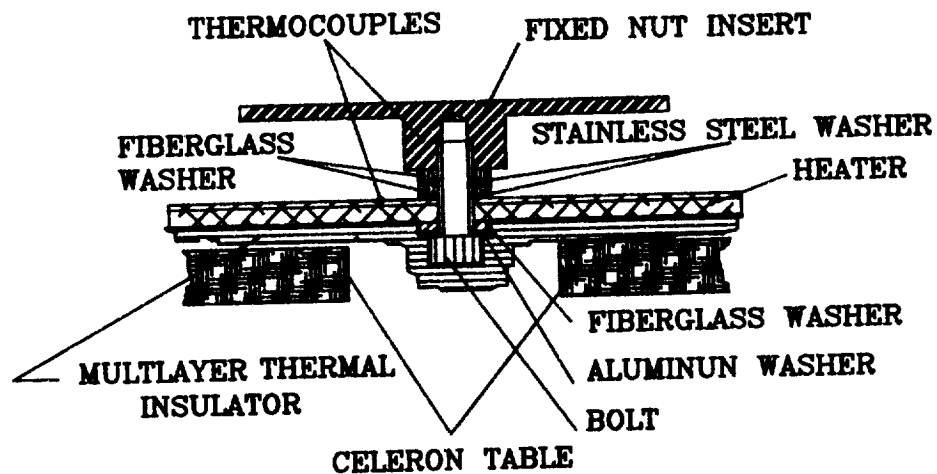


Figure 2. Fixed nut insert joint experimental apparatus

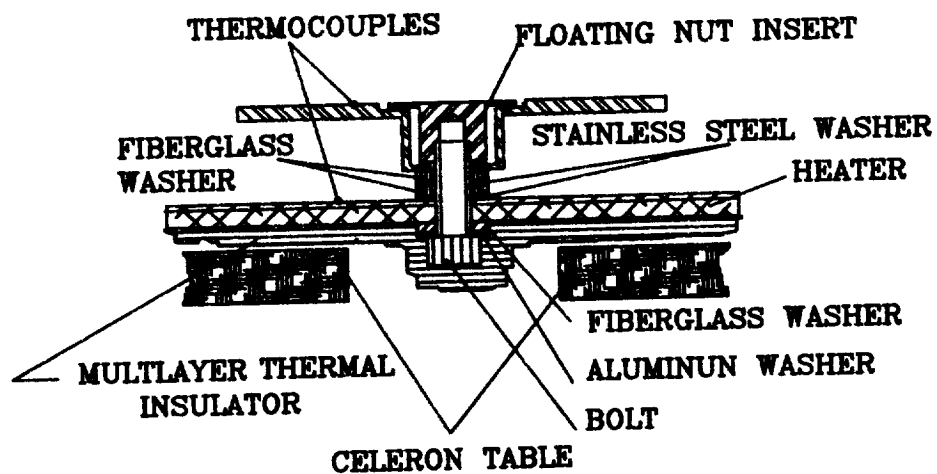


Figure 3. Floating nut insert joint experimental apparatus.

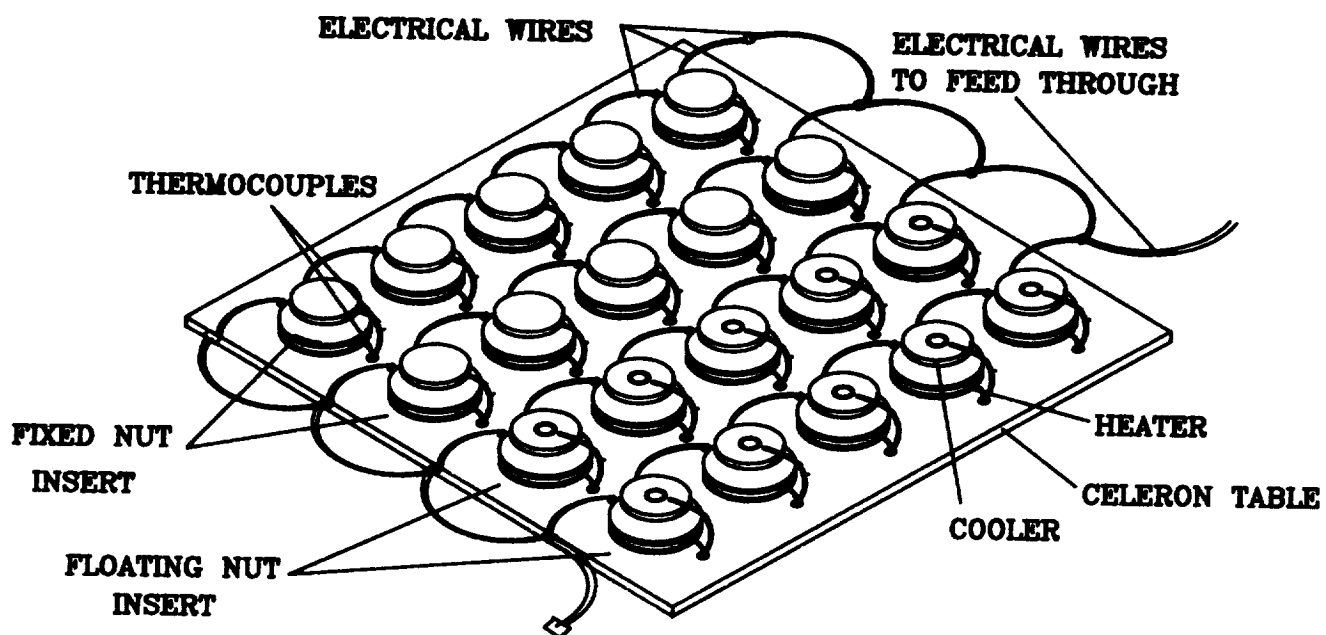


Figure 4. Final experimental mounting in Celeron table.

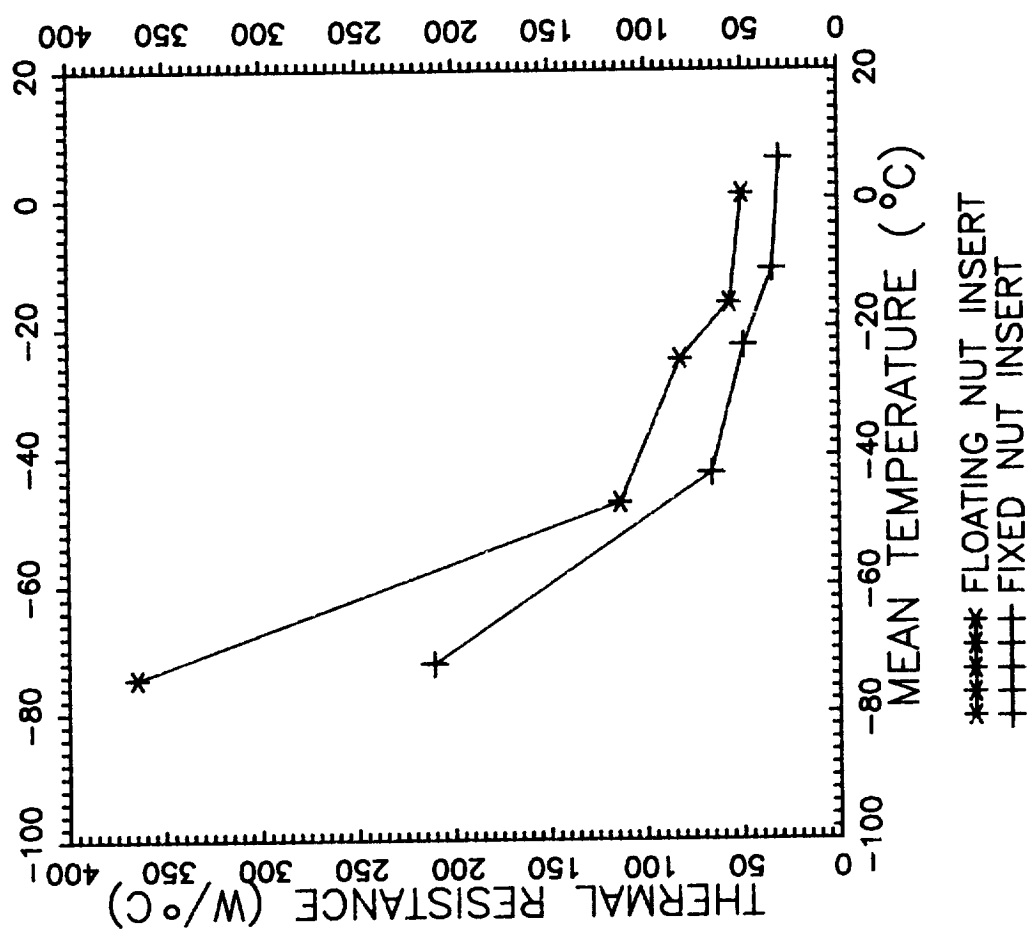


Figure 5. Thermal resistance as a mean temperature function for the two studied joints.

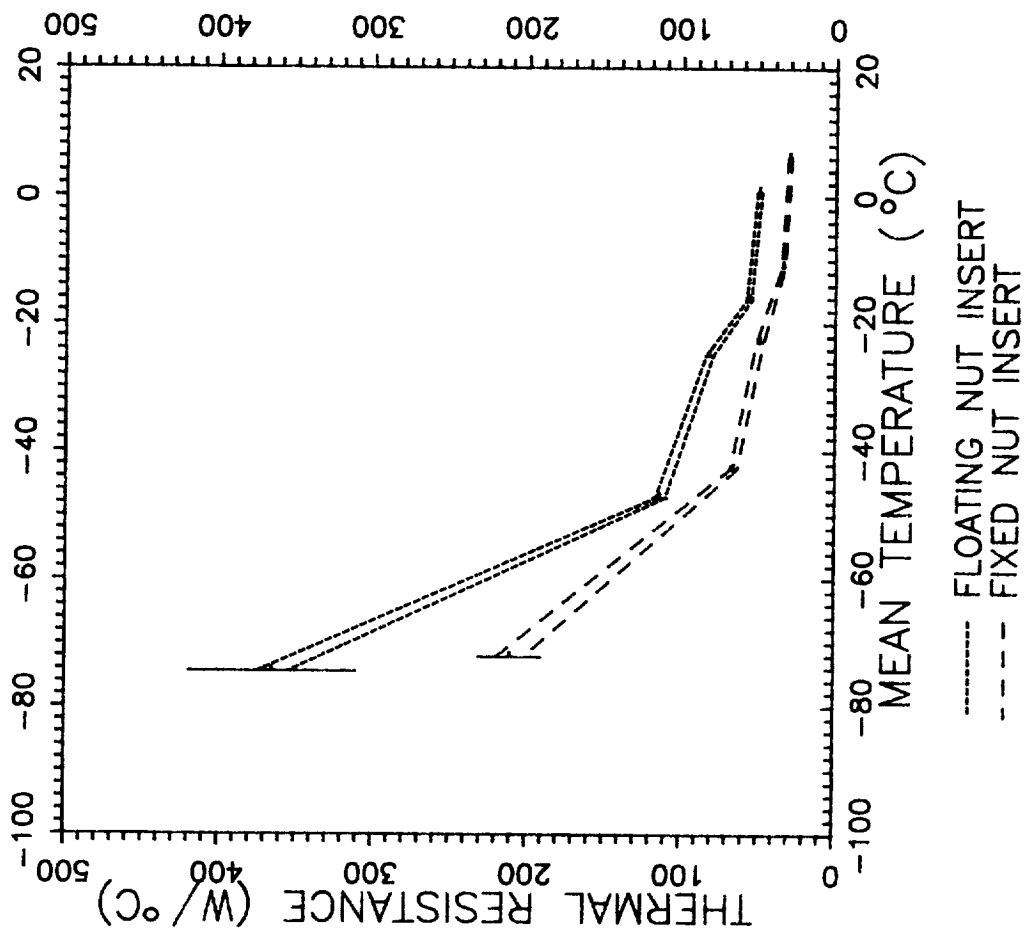


Figure 6. Thermal resistance as a mean temperature function with its associated experimental and standard errors.